The Fifteenth International Symposium on Artificial Life and Robotics 2010 (AROB 15th '10),
B-Con Plaza, Beppu,Oita, Japan, February 4-6, 2010

Robust Ride Comfort Control of vehicles without Measurements of Tire Deflection

Katsuhiro Okumura , Masahiro Oya and Hideki Wada

Fukuoka Industrial Technology Center, 3-6-1 Norimatsu, Yahatanishi-ku, Kitakyushu-shi, Fukuoka, Japan
(Tel: +81-93-691-0260; Fax: +81-93-691-0252) (E-mail: kokumura@fitc.pref.fukuoka.jp)
Department of Mechanical and Control Engineering, Kyushu Institute of Technology
1-1 Sensui-cho, Tobata-ku, Kitakyushu-shi, Fukuoka, Japan
Shin-Nippon Nondestructive Inspection Co., Japan, 4-10-13, Ibori, Kokurakita-ku, Kitakyushu-shi, Fukuoka, Japan

Abstract: In this paper, a robust ride comfort control scheme for vehicles is proposed in which the measurements of the tire deflections are not required. The controller has good property that we can specify a location where the ride comfort becomes best. To achieve this end, an estimator for the tire deflections and the road disturbances is proposed. Next, a combined ideal vehicle is designed. In the ideal vehicle, the location where ride comfort becomes best can be moved by setting only one design parameter. Finally, to force the real vehicle track the motion of the combined ideal vehicle, a robust tracking controller is designed.

Keywords: Vehicle, Ride comfort, Active suspension, Robust Tracking Control, Ideal Model

I. INTRODUCTION

Recently, in order to achieve good ride and good handling qualities, a large amount of control schemes using active suspensions have been proposed in [1]-[10]. In the case of realizing the best ride comfort at every location on a vehicle body, it must be required that the vertical acceleration and the angular acceleration of the vehicle body must be controlled so as to be zero. Then, some serious problems arise. For example, the suspension stroke may over an admitted range and the handling qualities may become worse. Therefore, in conventional schemes [1]-[10], the active suspensions are controlled so that the suspension strokes lie within an admitted range and the handling quality does not become worse. As a result, the ride comfort becomes best at only one specified location on the vehicle body. In case when the specified location has to be moved, the conventional active suspension controllers require a trial and error method, and then, too much time is spent to redesign an active suspension controller.

To struggle with the problem stated above, the authors have proposed schemes [11] [13]. In vehicle systems using the active suspension controllers proposed in [11]-[13], there exist good properties as follows: 1) The ride comfort at a specified location becomes best, 2) The best location can be easily moved by setting only one design parameter without redesigning a different suspension controller. However, in the proposed schemes [11]-[13], it is assumed that the tire deflections can be measured. Since the road surfaces are uneven, using non-contact sensors such as laser position sensors, it is difficult to measure the tire deflections with high accuracy.

In this paper, to overcome the problem stated above, a robust ride comfort control scheme is proposed. In the proposed controller, active suspensions are used as actuators and the measurements of tire deflections are not required. To realize good ride comfort without using the measurements of the tire deflections, we propose estimation methods for the tire deflections and the accelerations of road disturbances. The road disturbances imply the displacement of road surfaces. Using the estimate of the accelerations of road disturbances, we can design a combined ideal vehicle proposed in [13], and then, a robust tracking controller can be also designed so that the real vehicle track the motion of the combined ideal vehicle. At last, numerical simulations are carried out to demonstrate of the proposed robust active suspension controller.

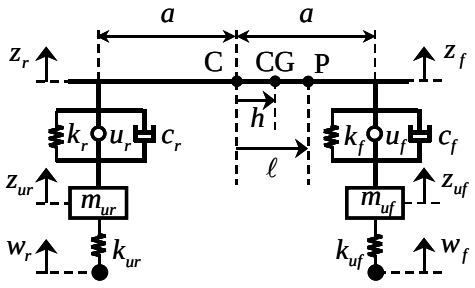

Fig. 1. Two wheels model.

II. VEHICLE MODEL

The two wheels model is shown in Fig. 1. The explanation of parameters is shown in Table 1. It is assumed that the pitching angle $\theta(t)$ is small, and then, the dynamic equation of vehicles is given as follows [7].

$$\left.\begin{array}{l} \ddot{\boldsymbol{x}}_z(t) = \boldsymbol{d}(t) \quad H^{\ 1}\ddot{\boldsymbol{w}}(t) \\ \ddot{\boldsymbol{x}}_u(t) = \quad K_u\boldsymbol{x}_u(t) \quad M_u^{\ 1}\boldsymbol{f}(t) \quad \ddot{\boldsymbol{w}}(t) \\ \boldsymbol{x}_z(t) = H^{\ 1}[z_f(t) \quad w_f(t) \ z_r(t) \quad w_r(t)]^T \\ \boldsymbol{x}_u(t) = [z_{uf}(t) \quad w_f(t) \ z_{ur}(t) \quad w_r(t)]^T \\ \boldsymbol{d}(t) = M^{\ 1}H^T\boldsymbol{f}(t) \\ \boldsymbol{f}(t) = [f_f(t) \quad f_r(t)]^T \\ \qquad = \quad C\dot{\boldsymbol{x}}_s(t) \quad K\boldsymbol{x}_s(t) + \boldsymbol{u}(t) \end{array}\right\} (1)$$

Table 1 Notation of vehicle model.

C CG	center and center of gravity of vehicle body
z_{cg} θ	vertical displacement at CG and pitching
z_f z_r	vertical displacement of vehicle body at positions on front and rear wheel axle
z_{uf} z_{ur}	vertical displacement of front and rear unsprung mass
w_f w_r	vertical displacement of road disturbance added to front and rear wheel
v	longitudinal velocity of vehicle
m i_c	sprung mass and moment of inertia of vehicle body
a	half of vehicle body length
h	distances from C to CG and from C to P
m_{uf} m_{ur}	front and rear unsprung mass
k_f k_r	front and rear suspension stiffness
c_f c_r	front and rear suspension damping rate
k_{uf} k_{ur}	front and rear tire spring stiffness
f_f f_r	front and rear force added to sprung mass
u_f u_r	front and rear active suspension control force

$$\left.\begin{array}{l} \boldsymbol{x}_s(t) = H\boldsymbol{x}_z(t) \quad \boldsymbol{x}_u(t) \\ \boldsymbol{u}(t) = [u_f(t)\ u_r(t)]^T \quad \boldsymbol{w}(t) = [w_f(t)\ w_r(t)]^T \\ M = (T_h^T)^{-1}\mathrm{diag}[m\ i_c]T_h^{-1} \\ M_u = \mathrm{diag}[m_{uf}\ m_{ur}] \quad K = \mathrm{diag}[k_f\ k_r] \\ C = \mathrm{diag}[c_f\ c_r] \quad K_u = M_u^{-1}\mathrm{diag}[k_{uf}\ k_{ur}] \\ T_h = I_2 \quad Dh\ H = \begin{bmatrix} 1 & a \\ 1 & -a \end{bmatrix} \quad D = \begin{bmatrix} 0 & 1 \\ 0 & 0 \end{bmatrix} \end{array}\right\} (2)$$

The control objective is to develop an active suspension controller so that the vertical acceleration at any specified location on the vehicle body can be reduced to a small value easily. To meet the objective, the following assumptions are made for actual vehicles considered here.

A1 The accelerations $\ddot{z}_f(t)$, $\ddot{z}_r(t)$, $\ddot{z}_{uf}(t)$ and $\ddot{z}_{ur}(t)$ are measured.

A2 The force $\boldsymbol{f}(t) = [f_f(t)\ f_r(t)]^T$ added to the sprung mass are measured.

A3 Suspension displacement $\boldsymbol{x}_s(t)$ and its velocity $\dot{\boldsymbol{x}}_s(t)$ are measured.

A4 Vehicle parameters are known except for the length a, the front and the rear tire stiffness k_{uf} k_{ur} and the tire mass m_{uf} m_{ur}.

A5 The second and third derivation of the road disturbance $\boldsymbol{w}(t)$ are bounded.

III. ESTIMATE OF STATE VARIBLES AND ROAD DISTURBANCE

Fig. 2 shows the configuration of the vehicle system proposed in [13]. The combined ideal model shown in Fig. 2 has good properties. Namely, 1) The ride comfort at a specified location becomes best, 2) The best location can be easily moved by setting only one design parameter without redesigning the combined ideal vehicle. If the real vehicle can track the motion of the designed combined ideal vehicle, the control objective can be achieved. The tracking controller in Fig. 2 is designed so that the real vehicle can track the motion of the combined ideal vehicle. To achieve control objective, the signals of road disturbance $\ddot{\boldsymbol{w}}(t)$ and state variables $\boldsymbol{x}_z(t)$, $\dot{\boldsymbol{x}}_z(t)$, $\boldsymbol{x}_u(t)$, $\dot{\boldsymbol{x}}_u(t)$ $\boldsymbol{d}(t)$ are required. According to assumptions, it can be seen that the following signals are available.

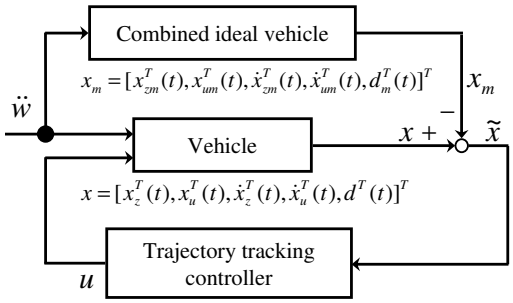

Fig. 2 Configuration of active suspension control system.

$$\left.\begin{array}{l} \ddot{\boldsymbol{x}}_s(t) = [\ddot{z}_f(t)\ \ddot{z}_r(t)]^T \quad [\ddot{z}_{uf}(t)\ \ddot{z}_{ur}(t)]^T \\ H\boldsymbol{d}(t) = [\ddot{z}_f(t)\ \ddot{z}_r(t)]^T \end{array}\right\} (3)$$

Moreover, it is easy from (1), (2) to ascertain that the following signals are also available.

$$\left.\begin{array}{l} \boldsymbol{p}_1(t) = K_u^{-1}\ \ddot{\boldsymbol{x}}_s(t) \quad (H\boldsymbol{d}(t) + M_u^{-1}\boldsymbol{f}(t)) \\ \qquad = \boldsymbol{x}_u(t) \\ \boldsymbol{p}_2(t) = \boldsymbol{x}_s(t) + \boldsymbol{p}_1(t) = H\boldsymbol{x}_z(t) \end{array}\right\} (4)$$

Since the signal $\dot{\boldsymbol{x}}_s(t)$ is available, if an estimator for $\dot{\boldsymbol{x}}_z(t)$ is developed, then, the signal $\dot{\boldsymbol{x}}_u(t)$ becomes also available. Therefore, we will develop an estimator for $\dot{\boldsymbol{x}}_z(t)$ and $\ddot{\boldsymbol{w}}(t)$. Let's consider the new state $\boldsymbol{\eta}(t) = [H\dot{\boldsymbol{x}}_z(t))^T\ \ddot{\boldsymbol{w}}(t)^T]^T$. Then, we have

$$\left.\begin{array}{l} \dot{\boldsymbol{\eta}}(t) = A\ \boldsymbol{\eta}(t) + \boldsymbol{q}_w(t) \\ A = \begin{bmatrix} O_2 & I_2 \\ O_2 & O_2 \end{bmatrix} \quad \boldsymbol{q}_w(t) = [0\ 0\ (\boldsymbol{w}(t)^{(3)})^T]^T \end{array}\right\} (5)$$

where O_n I_n denote n n zero matrix and n n unit matrix. Based on the relation (5), the estimator for the state $\boldsymbol{\eta}(t)$ is proposed as

$$\left.\begin{array}{l} \widehat{\boldsymbol{\eta}}(t) = (2\ C \quad 3\ ^2B\ )\boldsymbol{p}_2(t) + \boldsymbol{\zeta}(t) \\ \dot{\boldsymbol{\zeta}}(t) = A\ \widehat{\boldsymbol{\eta}}(t) \quad (2\ C \quad 3\ ^2B\ )C^T\widehat{\boldsymbol{\eta}}(t) \\ \boldsymbol{\zeta}(0) = \quad (2\ C \quad 3\ ^2B\ )\boldsymbol{p}_2(0) \\ B = [O_2\ I_2]^T \quad C = [I_2\ O_2]^T \end{array}\right\} (6)$$

where is a positive deign parameter introduced to improve performance of the proposed estimator. Defending the estimated error $\widetilde{\boldsymbol{\eta}}(t)$ as

$$\widetilde{\boldsymbol{\eta}}(t) = \begin{bmatrix} I_2 & O_2 \\ O_2 & -^1I_2 \end{bmatrix} (\boldsymbol{\eta}(t) \quad \widehat{\boldsymbol{\eta}}(t)) \qquad (7)$$

and differentiating the first equation in (6), we obtain the following the error equation.

$$\dot{\widetilde{\boldsymbol{\eta}}}(t) = \quad A_E\widetilde{\boldsymbol{\eta}}(t) + \quad ^1\boldsymbol{q}_w(t) \quad A_E = \begin{bmatrix} 2I_2 & I_2 \\ 3I_2 & O_2 \end{bmatrix} (8)$$

Table 2 Nominal values of parameters.

m	781	kg	i_c	990	kgm^2
h	0.04	m	a	1.38	m
k_f	27160	N m	k_r	29420	N m
c_f	4000	Ns m	c_r	2500	Ns m
m_{uf}	69	kg	m_{ur}	96	kg
k_{uf}	229000	N m	k_{ur}	255000	N m

For the proposed estimator, the following theorem holds

Theorem 1: For estimated errors $C^T\widetilde{\boldsymbol{\eta}}(t)$ and $B^T\widetilde{\boldsymbol{\eta}}(t)$, there exist bounded positive constants $^{-}_{Ei}$ $i = 1$ 2 independent of the design parameter such that

$$\|C^T\widetilde{\boldsymbol{\eta}}(t)|^2 \leq {}^{-}_{E1} \quad {}^{4} \quad \| \quad B^T\widetilde{\boldsymbol{\eta}}(t)\|^2 \leq {}^{-}_{E2} \quad {}^{2} \quad (9)$$

Proof of Theorem1: Since the system matrix A_E is asymptotically stable, Lyapnov equation

$$A_E^T P + PA_E = \quad 2I_4 \qquad (10)$$

has the positive definite matrix solution P. Then, differentiating the positive definite function $V(t) = \widetilde{\boldsymbol{\eta}}(t)^T P\widetilde{\boldsymbol{\eta}}(t)$, we have

$$\dot{V}(t) \leq \quad \frac{}{\max[P]}V(t) + \quad {}^{3} \quad {}_{w} \qquad (11)$$

where $_{w}$ is a positive constant value independent of the design parameter . Using the relation above, the inequalities in (9) can be derived.

It can be concluded from theorem 1 that estimated errors decrease as the design parameter increases. In case when the design parameter is set to be large enough, we can obtain the signals $\ddot{\boldsymbol{w}}(t)$ and $H\dot{\boldsymbol{x}}_z(t)$ with enough accuracy. Then, the signal $H\dot{\boldsymbol{x}}_z(t)$ $\dot{\boldsymbol{x}}_s(t) = \dot{\boldsymbol{x}}_u(t)$ becomes also available.

To demonstrate of the usefulness of the proposed estimator, numerical simulations are carrying out. Values of vehicle parameters are shown in Table 2. The vehicle velocity is set as $v = 100 \quad 1000$ 3600[m s]. Fig. 3 (a) shows the road disturbance $w_f(t) = w_r(t \quad L) \quad L = 2a \quad v$ and Fig. 3 (b) shows the disturbance $w_{nd1}(t)$ added to the measurement of $\boldsymbol{c}^T\boldsymbol{d}(t) \quad \boldsymbol{c} = [1 \quad 0]^T$. It is assumed that the disturbance $w_{nd1}(t)$ appears due to measurement accuracy of acceleration sensors and the maximum measurement error is 0 1m/s ^{2}.

At first, in case of using measurements without disturbances, we show responses of the velocity $y_z(t) = \boldsymbol{c}^T C\ \boldsymbol{\eta}(t)$, the road disturbance $y_w(t) = \boldsymbol{c}^T B\ \boldsymbol{\eta}(t)$, the estimated errors $\widetilde{y}_z(t) = \boldsymbol{c}^T C\ \widetilde{\boldsymbol{\eta}}(t)$ and $\widetilde{y}_w(t) = \boldsymbol{c}^T B\ \widetilde{\boldsymbol{\eta}}(t)$ in Fig. 4. As shown in Fig. 4, the estimated errors become small as the design parameter increases. Next, in the case of using measurements with disturbances, we show responses of the estimated errors $\widetilde{y}_z(t)$ and $\widetilde{y}_w(t)$ in Fig. 5. In this case, the design parameter is set as $= 2000$ and similar disturbances shown in Fig. 3 (b) are added in all measurements of acceleration sensors and force sensors. As shown in Fig. 5, also in the case of using measurements with disturbances, it is seen that estimated errors do not become large and available estimated signals can be obtained.

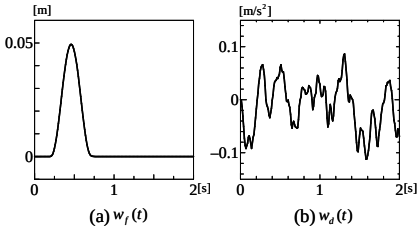

Fig. 3 Road disturbance $w_f(t)$ and disturbance $w_{nd1}(t)$ added to measurement $\boldsymbol{c}^T\boldsymbol{d}$.

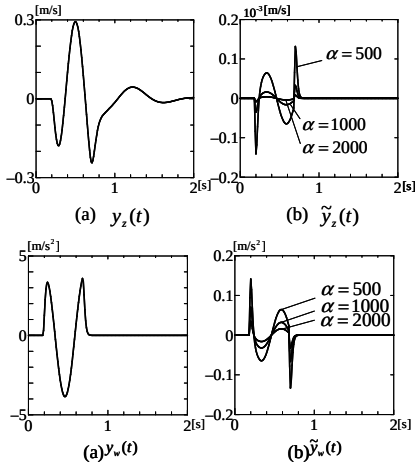

Fig. 4. Responses of $y_z(t)$, $y_w(t)$ and $\widetilde{y}_z(t)$, $\widetilde{y}_w(t)$.

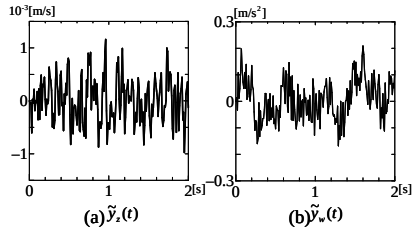

Fig. 5 Responses of $\widetilde{y}_z(t)$, $\widetilde{y}_w(t)$ in the presence of measurement disturbances.

IV. TRACKING CONTROLLER

Fig. 6 shows the vehicle system using estimates proposed in the previous section. The stability and good tracking performance of the vehicle system can be shown by using the similar manner stated in [13].

V. NUMERICAL SIMULATION RESULTS

The numerical simulation results are shown to confirm usefulness of the proposed robust active suspension controller. The values shown in Table 2 are used as nominal values for vehicle parameters, and the vehicle velocity is set as $v = 100 \quad 1000$ 3600m s. The combined ideal vehicle designed in [13] is used. The design parameters are set as $= 2000$ $\gamma = 100$. The design parameter γ is the feed back gain introduced in [13] to force the actual vehicle track the motion of the combined ideal vehicle. Fig. 7 shows the maximum gain curves of the nominal vehicle controlled so that the real vehicle can track the motion of the combined ideal vehicle. The thin lines show the maximum gain curves of the controlled nominal vehicle, the

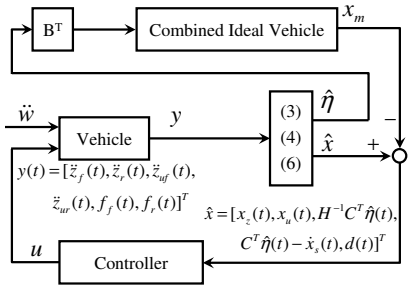

Fig. 6 Configuration of the vehicle system using estimates.

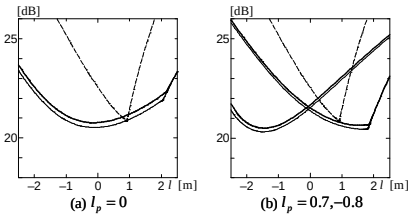

Fig. 7 Maximum gain curves of the controlled nominal vehicle.

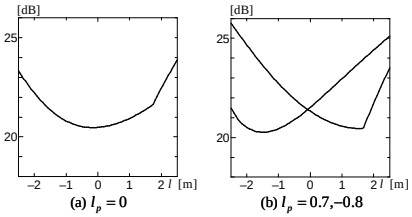

Fig. 8. Maximum gain curves for variations of $K\ C$.

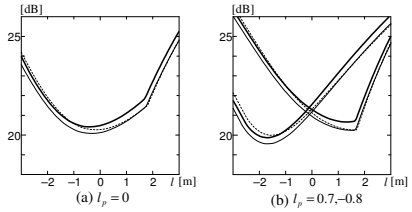

Fig. 9. Maximum gain curves for variations of M.

thick lines show the maximum gain curves of the combined ideal vehicle, and the dashed lines show the nominal vehicle without control. It is seen from Fig. 7 that the maximum gain curves are mostly same between the combined ideal vehicle and the controlled nominal vehicle. It is also seen that the location where the ride comfort becomes best can be easily moved by setting only one design parameter $_p$. The design parameter $_p$ is introduce to move the location where the ride comfort becomes best in the combined vehicle model proposed in [13].

Fig. 8 shows the maximum gain curves of the controlled vehicle with the parameter uncertainties $(K\ C) = (\overline{K}\ \overline{C})\ (0\ 8\overline{K}\ 0\ 8\overline{C})\ (1\ 2\overline{K}\ 1\ 2\overline{C})$. The thick lines show the maximum gain curves of the controlled nominal vehicles, and the thin lines show the maximum gain curves of the controlled vehicle with parameter uncertainties. There is no difference for variations of $K\ C$.

Fig. 9 shows the maximum gain curves of the controlled vehicle with the parameter uncertainties $(m\ i_c\ h) = (\overline{m}\ \overline{i}_c\ \overline{h})\ (0\ 8\overline{m}\ 0\ 8\overline{i}_c\ \overline{h}\ +\ 0\ 3)\ (1\ 2\overline{m}\ 1\ 2\overline{i}_c\ \overline{h}\ +\ 0\ 3)$. The thick lines, dashed lines, and thin lines show the each results with the parameter$(m\ i_c\ h) = (\overline{m}\ \overline{i}_c\ \overline{h})\ (0\ 8\overline{m}\ 0\ 8\overline{i}_c\ \overline{h}+0\ 3)\ (1\ 2\overline{m}\ 1\ 2\overline{i}_c\ \overline{h}+0\ 3)$. It can be seen that some differences appear between the controlled vehicle with uncertainties and the controlled nominal vehicle but small enough.

VI. CONCLUSION

We have proposed the active suspension control scheme in which tire deflections are not required. The proposed suspension controller has a good property that the location where the ride comfort becomes best can be easily moved by setting only one design parameter $_p$. It has been shown by carrying out numerical simulations that ride comfort becomes best at the specified location even if there are uncertainties in the suspension stiffness k_f, k_r, damping rate c_f, c_r, the sprung mass and the moment of inertia $m\ i_c$ and the distance h from C to CG.

REFERENCES

[1] D. Hrovat, Survey of Advanced Suspension Developments and Related Optimal Control Application, *Automatica*, Vol.33-10, pp.1781-1817, (1997).

[2] A.G. Thompson and B.R. Davis, RMS values for control force, suspension stroke and tire deflection in an active suspension, *Vehicle System Dynamics*, Vol. 34, pp. 143-150, (2000).

[3] A.G. Thompson and C.E.M. Pearce, Performance index for a preview active suspension applied to a quarter-car model, *Vehicle System Dynamics*, Vol. 35, No. 1, pp. 55-66, (2001).

[4] A.G. Thompson and C.E.M Pearce, Direct computation of the performance index for an optimally controlled active suspension with preview applied to a half-car model, *Vehicle System Dynamics*, Vol. 35, No. 2, pp. 121-137, (2001).

[5] L. Wenger and F. Borrelli, The application of constrained optimal control to active automotive suspensions, *Proceedings of IEEE Conference on Decision and Control*, pp. 881-886, (2002).

[6] L. Zuo and S.A. Nayfeh, Structured H_2 optimization of vehicle suspensions based on multi-wheel models, *Vehicle System Dynamics*, Vol. 40, No. 5, pp. 351-371, (2003).

[7] J.-S. Lin and C.-J. Huang, Nonlinear backstepping active suspension design applied to a half-car model, *Vehicle System Dynamics*, Vol. 42, No. 6, pp. 373-393, (2004).

[8] H. Chen and C.W. Scherer, An LMI based model predictive control scheme with guaranteed H_∞ performance and its application to active suspension, *Proceedings of the American Control Conference*, pp.1487-1492, (2004).

[9] H. Chen and K.-H. Guo, Constrained H_∞ control of active suspensions: An LMI approach', *IEEE Trans. Control System Technology*, Vol. 13, No. 3, pp. 412-421, (2005).

[10] H. Nishimura and N. Takahashi, Active Vibration Control for Suspension by Consideration Its Stroke Limitation, *Journal of System Design and Dynamics*, Vol.1, No.2, pp.138-146, (2007).

[11] M. Oya, H. Harada, Y. Araki, An Active Suspension Controller Achieving the Best Ride Comfort at Any Specified Location on A Vehicle, *Journal of System Design and Dynamicss*, pp.245-256, (2007).

[12] H. Okuda, Y. Tsuchida, M. Oya, Q. Wang, and K. Okumura, Robust Active Suspension Controller Achieving Good Ride Comfort, Proc. of SICE Annual Conference 2007, September 17-20, Kagawa, Japan, pp. 1305-1310, (2007).

[13] M. Oya, Y. Tsuchida, Q. Wang, Y. Taira, Adaptive Active Suspension Controller Achieving the Best Ride Comfort at Any Specified Location on Vehicles with Parameter Uncertainties, *International Journal of Advanced Mechatronic Systems*, Vol. 1, No. 2, pp. 125-136, (2008).